Available online at www.sciencedirect.com
SCIENCE DIRECT®
European Journal of Medicinal Chemistry 40 (2005) 75–83
EUROPEAN JOURNAL OF MEDICINAL CHEMISTRY
www.elsevier.com/locate/ejmech

Original article

Homology models of the cannabinoid CB1 and CB2 receptors. A docking analysis study

Cristina Montero, Nuria Eugenia Campillo, Pilar Goya, Juan Antonio Páez *

Instituto de Química Médica (CSIC), Juan de la Cierva 3, 28006 Madrid, Spain

Received 16 December 2003; received in revised form 15 July 2004; accepted 5 October 2004

Available online 26 November 2004

Abstract

The 3D models of both CB1 and CB2 human receptors have been established by homology modeling using as template the X-ray structure of bovine Rhodopsin (code pdb: 1F88) a G-protein-coupled receptor (GPCR). A recursive approach comprising sequence alignment and model building was used to build both models, followed by the refinement of non-conserved regions. The cannabinoid system has been studied by means of docking techniques, using the 3D models of both CB1 and CB2 and well known reference inverse agonist/antagonist compounds. An approach based on the flexibility of the structures has been used to model the receptor–ligand complexes. The structural effects of ligand binding were studied and analyzed on the basis of hydrogen bond interactions, and binding energy calculations. Potential interaction sites of the receptor were determined from analysis of the difference accessible surface area (DASA) study of the protein with and without ligand.

Keywords: Cannabinoid receptor; CB1; CB2; G-protein-coupled receptors (GPCRs); Homology modeling; Docking

1. Introduction

Cannabinoid receptors interact with cannabinoid drugs including the classical cannabinoids such as Δ^9-tetrahydrocannabinol (Δ^9-THC) that is the main psychotropic constituent of cannabis, their synthetic analogs and with the endogenous cannabinoids [1–4]. The potential therapeutic applications claimed for cannabinoid receptor agonists include attenuation of nausea and vomiting in cancer chemotherapy, management of glaucoma, the suppression of muscle spasticity/spasm associated with multiple sclerosis and spinal cord injury, disorders associated with Alzheimer's disease [5,6] and therapeutical effects of analgesia [7–11]. CB1 receptor antagonists/inverse agonists have potential therapeutic application as appetite suppressants [12–14] and in the management of schizophrenia [15]. The side effects accompanying these therapeutic responses include alterations in cognition and memory, dysphoria, euphoria, and sedation [16].

There are two types of cannabinoid receptors that have so far been identified, CB1 cloned in 1990 [17], and CB2 cloned in 1993 [18]. The CB1 cannabinoid receptor has been cloned from rat [17], mouse [19], and human [20,21] tissues and shows 97–99% amino acid sequence identity across species and it is found primarily in brain and neuronal tissue, whereas CB2 is found mainly in immune cells where they may mediate an immunosuppresant effect. The CB2 cannabinoid receptor shows 44% identity with the CB1 cannabinoid receptor [18]. At present, there is some preliminary pharmacological evidence that supports the existence of additional types or subtypes of cannabinoid receptors [22–24].

Both cannabinoid receptor types belong to the large family of G-protein-coupled receptors (GPCRs) [25] controlling a wide variety of signal transduction. In addition, CB1 receptors are also coupled through G-proteins to several types of calcium and potassium channels. GPCRs are a large superfamily, which are integral membrane proteins that are characterized by seven hydrophobic transmembrane helices (TMH). Therefore, the knowledge of the structural features of cannabinoid receptors is of the utmost importance for the understanding of their function and for their use for drug design. For theses purposes, in the last decade, the structures used as template in the molecular modeling studies of

* Corresponding author. Tel.: +34 91 562 2900; fax: +34 91 564 4853.
E-mail address: juan@suricata.iqm.csic.es (J.A. Páez).

0223-5234/$ - see front matter © 2004 Elsevier SAS. All rights reserved.
doi:10.1016/j.ejmech.2004.10.002

GPCRs have been based on the structure of bacteriorhodopsine (BR) [26] or in low-resolution crystal structures of GPCRs. The ground state of Rhodopsin was determined at 2.8 Å resolution by X-ray crystallography [27] and NMR [28,29]. This experimental result has allowed to undertake the modeling of the GPCRs with greater reliability. Therefore, we have used this structure as suitable template to build by homology modeling 3D models of both CB1 and CB2 receptors.

Identification of the binding site and binding conformations of cannabinoid ligands within the CB receptors is of great interest for the understanding of principles that account for the interactions between the ligand and the amino acid residues and for the design of new ligands. Site-specific mutation studies on the Rhodopsin subfamily of receptors suggest that the ligand binding site is localized within the TM core region in the crevice formed by TM3, TM5, TM6, and TM7 [27,30].

Ligand design represents an integral approach useful to provide structural information not available from the experiment methods. Docking studies have been used to study the binding orientations and prediction of binding affinities.

Classical cannabinoids are tricyclic terpenoid derivatives bearing a benzopyran moiety. This class includes the natural product (–)Δ^9-THC and other pharmacologically active constituents of the plant *Cannabis sativa*. A second class of cannabimimetics was developed at Pfizer which includes bicyclic (e.g. CP55940) and tricyclic (e.g. CP55244) analogs lacking the pyran rings of classical cannabinoids (Fig. 1). The diarylpyrazoles are another type of cannabinoid analogs, one of them is SR141716A developed by Sanofi which is currently in clinical phase for the treatment of obesity and addictions. The other diarylpyrazol is SR144528 developed by Sanofi which is a potent and selective CB2 receptor ligand. A second chemical class of cannabinergics are the aminoalkylindoles that were developed at Sterling Winthrop as potential non-steroidal anti-inflamamatory agents. WIN55212-2 is a potent CB1 and CB2 agonist with high stereoselectivity and a slight preference for CB2. AM-630 is the first CB2-selective antagonist derived from this class of compounds [1] (Fig. 2).

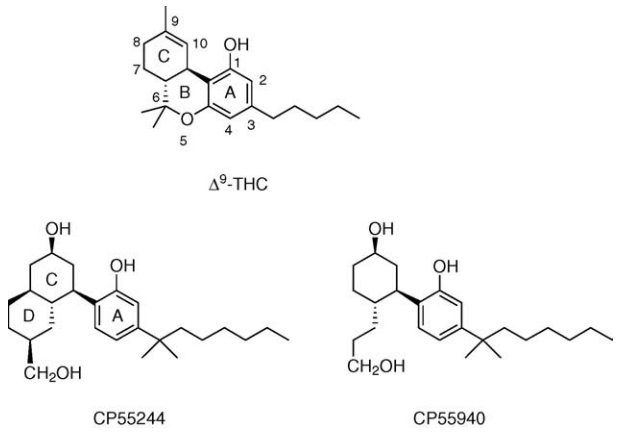

Fig. 1. Cannabinoid CB1 and CB2 receptor ligands analog of Δ^9-THC.

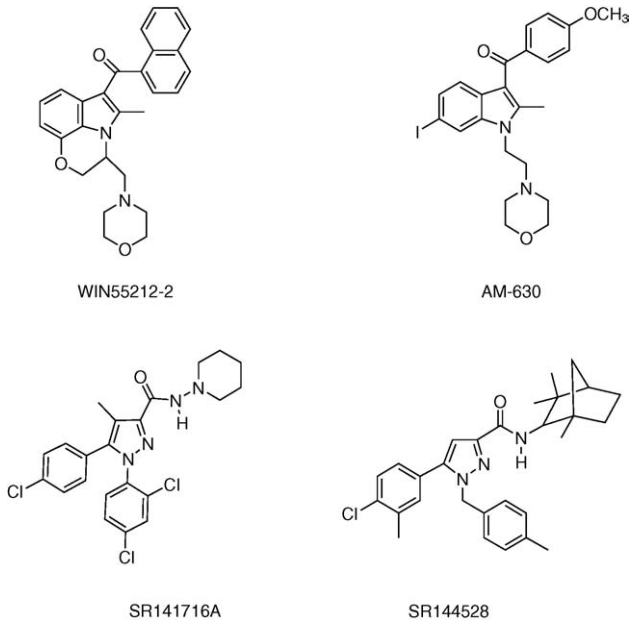

Fig. 2. Cannabinoid receptor ligands analog of WIN55212-2 and SR-141716 A.

In the present study, a homology model of the CB1 and CB2 receptor was constructed using the X-ray crystal structure of bovine Rhodopsin as the structural template. A molecular docking approach with FlexiDock [31] was employed to identify the binding site in CB1 and CB2 receptors from representative inverse agonist or antagonist ligands (Fig. 2).

2. Computational methods

2.1. Homology model of the CB1 and CB2 receptor

The modeling process by homology consists in several steps essential for obtaining a correct sequence alignment of the target sequences CB1 and CB2 with the homologous visual Rhodopsin (Rho) in the inactivated state (code PDB: 1F88) used as basic structure. The approach followed was developed and improved by Burke et al. [32]. The sequential alignment of Rhodopsin and the cannabinoid receptor CB1 and CB2 was performed using the sequence alignment program CLUSTALW [33] followed by a manual adjustment of the multiple alignment sequence with the program SEAVIEW [34] and formatted using the program JOY [35].

From the best alignment, 3D models containing all non-hydrogen atoms were obtained automatically using the method implemented in MODELLER [36,37]. Based on the sequence alignments, MODELLER extracts a large number of spatial restraints from the template structures and builds a molecular model of the query protein. The restraints are generally obtained by assuming that the corresponding distances and angles between aligned residues in the template and the target structures are similar. A 3D model is obtained by optimization of a molecular probability density function (pdf). Minimization of the models was performed automati-

cally by the program using the Charmm force field, using the conjugate gradient method with a convergence gradient of 0.01. The models had to satisfy most restraints used to calculate them, particularly those concerning their stereochemistry. Of the 15 models generated with MODELLER, the one corresponding to the lowest value of the pdf and fewest restraints violations was used for further analysis. The resulting molecular models were validated and the cycle of realignment, modeling and structure validation was repeated until no further improvement on the structure was observed.

The structurally variable regions (SVRs) as loops were built with the standard procedure in MODELLER and afterwards they were refined. For short loops the MODELLER procedure gives good results and in this case, the loops available from the parent structure were selected. Long loops were refined using the Search-Loop option in the SYBYL program [31] software suite coupled database. This database has been built from a large set of high-resolution protein structural fragments. The 25 loops found by SYBYL were clustered in families. Each family was analyzed in order to identify sequence and number of the Van der Waals contacts ; thus, for each receptor the fragment that was located between two anti-parallel helical elements and which showed an identity sequence over 25 % and with the lower number of the Van der Waals contacts was chosen. Both final models were minimized with the minimizing option of SYBYL using the Kollman All atom force field and Kollman charges in order to avoid the unfavored possible contacts. After the refinement process the models were validated using the VERIFY [38], PROCHECK [39] and COMPARER [40,41] programs.

2.2. Molecular docking of cannabinoid compounds

The structures of the ligands were built with standard bond lengths and angles using the molecular modeling package SYBYL and their energies were minimized using the Powel method with a conjugated gradient of <0.001 kcal/mol convergent criteria provided by the Tripos force field [42] and electrostatic charges based on the method of Gasteiger-Hückel.

Conformational studies for the considered ligands were carried out taking into account the studies published and the minimized structures were initially placed in the inactivated state of the cannabinoid receptors CB1 and CB2 according to literature data [43–48]. SR141716A was manually positioned within the TMH 3-4-5-6 aromatic microdomain of cannabinoid receptor. This region includes the aromatic residue F3.25, F3.36, W4.64, Y5.39, W5.43 and W6.48. Three of these amino acids, F3.36, W5.43 and W6.48 were found in a recent mutation and computational study of the CB1 receptor [49] to form a triad of interacting aromatic residues in the CB1 receptor which would be available for ligand binding. The aminoalkylindoles bind in the same aromatic microdomain. It has been hypothesized that aromatic stacking, rather than hydrogen bonding interactions, is the primary interaction for the AAIs at CB1 [48,50].

This binding pocket was the starting point to calculate with ligand protein contact (LPC) server [51] additional interactions available between the ligand and the receptor. The ligand–receptor complex was subjected to energy minimization using the Tripos force field and electrostatic charges of Gasteiger-Hückel and their energies were minimized using the protocol previously indicated.

These complexes were the input structure for docking using Flexidock command in the Biopolymer module. FlexiDock software performs flexible docking of conformationally flexible ligands into receptor binding sites and provides control of ligand binding characteristics, taking into account rigid, partially flexible, or fully flexible receptor side chains. FlexiDock incorporates the Van der Waals, electrostatic, torsional and constraint energy terms of the Tripos force field, and it uses a genetic algorithm (GA) to determine the optimum ligand geometry. GA borrow methodology and terminology from biological (or Darwinian) evolution, in that they are an iterative process in which the most-fit members of a population will have the best chance of propagating themselves into future generations [52].

During the flexible docking analysis, the protein was considered rigid except the residues involved in the binding site and the ligands were considered flexible. The default SYBYL FlexiDock parameters were utilized in all cases, with iterations set to 30,000 obtaining a series of model complexes.

After visual examination of the output complexes of Flexidock, the complexes were analyzed on the basis of the score provided by Flexidock and the interaction between ligand–receptor with LPC. We have chosen the conformation with the lowest score and fulfilling the experimental requirements.

The docking study of the CB2 receptor with different ligands was performed in analogous way to the CB1 receptor.

3. Results and discussion

3.1. Homology modeling

Multiple Sequence Alignment. Sequentially, CB1 and CB2 share 21% and 20% of identity with visual Rhodopsin (code pdb: 1F88) and only 44% between CB1 and CB2. Fig. 3 shows a schematic representation of the cannabinoid receptors. Residues highly conserved in the GPCR family are shown in Table 1.

The sequential alignment of Rhodopsin and cannabinoid receptors is shown in Fig. 4. Most of the key residues characteristic of GPCRs are conserved in CB1 and CB2. The major sequence differences between 1F88 and the cannabinoid receptors lie in the transmembrane region TM5. The GPCR family has a highly conserved proline in TM5 (215, 1F88 numbering) whereas it is not present in the cannabinoid receptor and additionally, two tyrosine residues (207 and 208, CB2 numbering) are present in CB1 and CB2 in a region

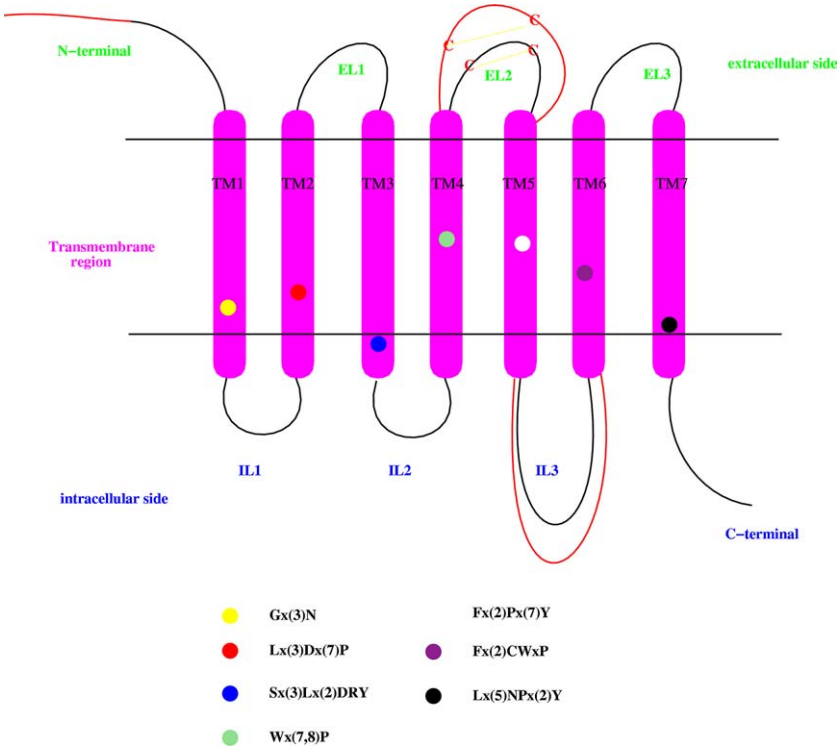

Fig. 3. Two-dimensional model of CB1 and CB2 receptor. The conserved patterns in the GPCR family are shown as color cycles. The red lines show the different length in these three areas.

Table 1
Key residues conserved in the GPCR family

TM	*Pattern*	*Rhodopsin*	*CB1*	*CB2*
TM1	Gx[a](3)N	+	Gx(2)Tx(3)N	Gx(2)Sx(3)N
TM2	Lx(3)Dx(7)P	Lx(3)D	Lx(3)D	Lx(3)D
TM3	Sx(3)Lx(2)Ix(2)DRY	+	Sx(3)Tx(2)Ix(2)DRY	Sx(3)Tx(2)Ix(2)DRY
TM4	Wx(7,8)P	+	+	+
TM5	Fx(2)Px(7)Y	+	–	–
TM6	Fx(2)CWxP	+	Lx(2)CWxP	Lx(2)CWxP
TM7	Lx(5)NPx(2)Y	Kx(5)YNPx(2)Y	+	+

[a] x, any residue.

normally containing a single tyrosine. In addition, this region shows in CB1 and CB2 a strong aromatic environment, more remarkable in CB2. Another important difference is the absence in CB1 and CB2 of the cysteines involved in a disulfide bridge present in all members of the GPCRs family. Nevertheless, there are two other cysteines conserved in both cannabinoid receptors that could be involved in a disulfide bridge [53].

On the other hand, the most important differences between CB1 and CB2 are located in the N-terminal, extracellular loop II (EL2), C-terminal of transmembrane helix VII (TM7) and the C-terminal. Only CB1 of all members of the class I of GPCR family has a long N-terminal, approximately of 70 residues and a search in PSI-BLAST [54] did not give any significant hit on this region. While the cannabinoid receptor CB2 shows a rich proline region in EL2, another feature of CB2 is the aromatic environment of TM5. CB1 has a serine (at position 317) located in the intracellular loop III (IL3) that is a phosphorylate site of protein kinase C (PKC) [55] whereas in CB2, this serine is not present. CB1 shows a region (RxAFRS) (Fig. 4) that is well conserved in cation channel receptors such as the vanilloid receptor VR1 [56].

3.1.1. Modeling of the core of the CB1 and CB2 receptors

The amino acids terminal domain of the CB1 receptor is uncommonly long among the various members of the class I GPCRs and it is crucial in the early steps in the biosynthesis of the receptor and may play a role in regulating the stability and surface expression of CB1 but seems to play no role in ligand recognition [57]; therefore, we modeled CB1 without the first 70 amino acids. The structurally conserved regions (SCRs) were modeled using the target sequence to structural template alignment (Fig. 4) as input to the program MODELLER using bovine Rhodopsine as template. The resulting output was a comparative model of CB1 and CB2. Evaluation of the stereochemical quality of the model with PROCHECK showed that only a few residues are in disallowed regions in the Ramachandran plot and most of them

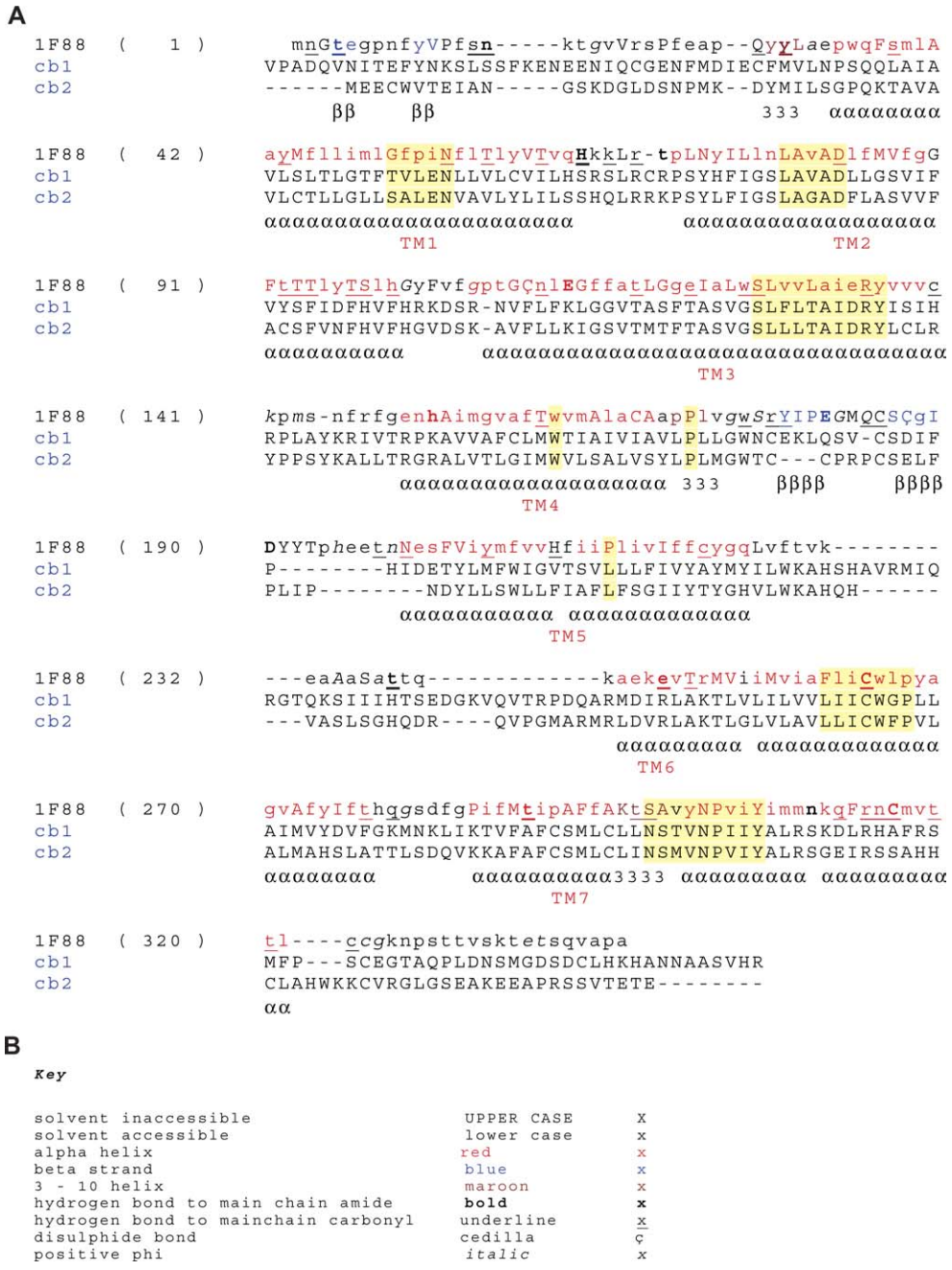

Fig. 4. (a) Sequence alignment of 1F88 (chain a) with the sequences of the CB1 and CB2. The conserved patterns are boxed. (b) Key to JOY alignment.

correspond to the structurally non-conserved regions. On the other hand, in all members of the GPCR family there is a disulfide bridge. As mentioned above, the cysteines involved in this disulfide bridge are not conserved in cannabinoid receptors, however, there are two other cysteines (Cys175 and Cys179; CB2 numbering) that could be involved in the formation of a disulfide bridge [53]. Thus, we studied on these theoretical models the possibility of the formation of a disulfide bridge. Of all the extracellular cysteines, only the formation of the disulfide bridge between the cysteines located in EL2 is possible due to the distances, in agreement with the published data [53]. Therefore, the models were built again with the extra restraints based on the formation of the disulfide bridge between the corresponding cysteines. These models show an improved Ramachandran plot and energy profile with respect to the initial models.

To examine the orientation of the helixes of CB1 and CB2, we superposed the transmembrane regions of the models with the template. From the root-mean-square (RMS) values for CB1 (0.65 Å) and CB2 (0.68 Å) we can conclude that there is a good agreement between the helices. The lengths of the seven TMH are nearly the same as it was expected for all members of this family.

Table 2 shows the sequence identity percentage of the TMH. Except for TM1 from CB2 and TM5 from CB1 and CB2, the percentage of identity with bovine Rhodopsin (pdb

Table 2
Identity percentage of TM (Rhodopsin, CB1 and CB2)

TM	*Rhodopsin (%CB1/%CB2)*	*CB1 (%CB2)*
TM1	25.8/45.2	25.8
TM2	23.3/16.7	70.0
TM3	22.6/25.8	71.0
TM4	21.1/15.8	26.3
TM5	9.1/4.5	27.3
TM6	17.4/21.7	69.6
TM7	17.6/17.6	61.8

entry 1F88) is around 20%. TM1 from CB2 shows the highest value (45.2%) while TM5 of both cannabinoid receptors show the lower values. On the other hand, the percentage of identity between CB1 and CB2 is around 70% except TM1, TM4 and TM5. This is in agreement with the fact that the selectivity of the substrates is located in these regions.

3.1.2. Modeling of the non-conserved regions

Once the models of the TM region of CB1 and CB2 were obtained, the next step was refining the non-conserved regions. Most of the loops are short and they matched well with the template (Fig. 4), because short loops generally have severe spatial restrictions due to their length.

There are only two SVRs with large insertion and deletion, EL2 and IL3. EL2 is involved in the binding of the substrates. The modelization of the EL2 was performed during the process of modeling of the backbone of CB1 and CB2. We defined disulfide bonds between Cys 187–194 (CB1) and Cys 174–179 (CB2).

It is worth mentioning that in EL2 from CB1 receptor there are two β-strands building up a β-sheet with the other two β-strands located in the N-terminal region.

Finally the loops IL3 of both receptors were refined using the Search-Loop option. IL3 plays an important role in the binding of G-proteins [58].

The IL3 in CB2 receptor is featured by well-defined helices forming the intracellular end of TM5 and TM6, whereas the central region is mostly unstructured, according to the prediction of secondary structure carried out with the program PREDATOR [59,60] and PHD [61]. Besides, the structure of the IL3 of CB1 was determined with NMR by Ulfers et al. [62], being consistent with our prediction.

About CB2, the region IL3 was modeled as extension of both helices, TMH5 and TMH6. This is in agreement with the prediction of secondary structure of this region.

Fig. 5. JOY output of the structural superposition of the CB1, CB2 models and 1F88a.

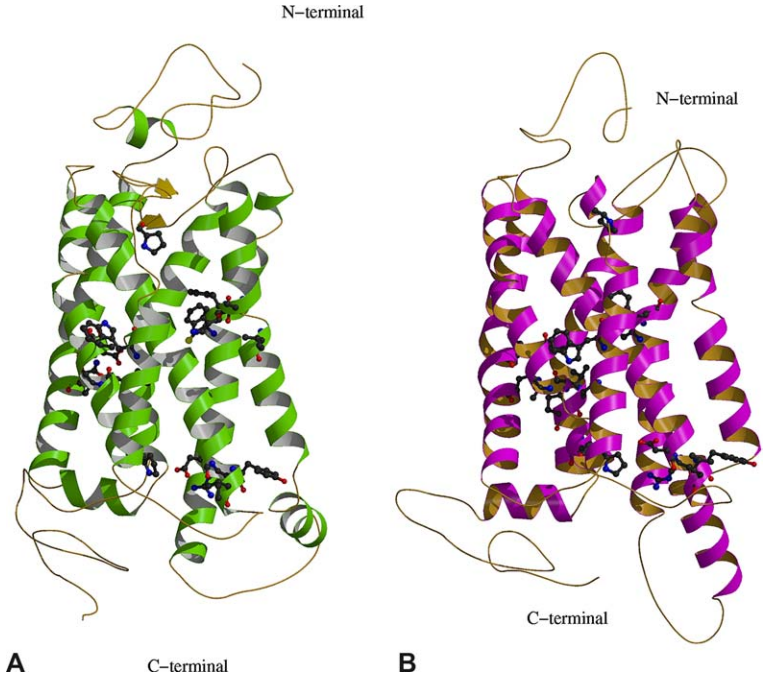

Fig. 6. The models of CB1 (A) and CB2 (B) receptors drawn as ribbon diagram. The conserved patterns are shown as ball-and-sticks models. Figure generated with Molscript [66] and Raster3D [67,68].

Both loop models were modeled as an extension of the helices into the cytoplasmatic face, this fact being in agreement with the data published by Yeagle et al. [30] who determined an experimental three-dimensional structure for Rhodopsin in the inactivated state for the IL3.

After the refinement process the models were validated using the VERIFY 3D and PROCHECK programs. The Ramachandran plot shows that only a few residues (3.8% in CB1 and 2.0% CB2) are in disallowed regions. The average score obtained with VERIFY 3D is 0.65 and 0.67 for CB1 and CB2, respectively, comparable with 0.70 of visual Rhodopsin. The JOY output and the final models are shown in Fig. 5 and Fig. 6, respectively.

3.2. Docking of the cannabinoid ligands

In order to investigate the predictivity as well as the characteristics of the binding site of our models and to facilitate the rational design of novel and more selective cannabinoid receptor ligands, docking analysis was performed on a set of well known ligands, inverse agonist and/or antagonist compounds with different selectivities towards CB1 and CB2 receptors (Fig. 2). Analysis of the receptor–ligand complex models generated after successful docking of the inhibitors was based on the hydrogen bond interactions, aromatic and hydrophobic interactions, energy of binding and the difference accessible surface area (DASA).

As a general rule, the interaction of the ligand with the cannabinoid receptor is mediated by specific hydrogen bond and aromatic interactions between the ligand main chain and the active site of the receptor [43,44,63]. Taking these facts into account, we have used hydrogen bond and aromatic interactions as the major criterion for analysis. Energy of binding was calculated for each receptor–ligand complex with DOCK program. Finally, the DASA study of a protein with and without ligand reveals the potential interaction sites of the protein to estimate the fit of contact between the protein and the ligand [64] (Table 4).

3.3. Docking of the cannabinoid ligands in CB1 and CB2 receptor

In Table 3 are gathered the residues involved in the first and second sphere of the binding site resulting of ligand–receptor CB1 and CB2 complexes studied.

Table 4 illustrates the key predicted LPC data for ligands besides the binding energy and the k_i values. Docking analysis reveal that the antagonist/inverse agonist SR141716A binds in the TM4-E2-TM5 region of the CB1 receptor (Table 4).

The interactions that account for the docking are a combination of hydrogen bonding and aromatic interactions predicted by LPC and DASA (Tables 3 and 4). SR141716A shows HB with K122 and aromatic interaction with W209 according to mutagenesis studies [65] that have shown the influence of this residue in the k_i value. Thus, the docking results show that SR141716A interact with residue in the TM4-E2-TM5 of CB1 through a combination of HBs and aromatic interactions.

A similar study has been performed in the CB2 cannabinoid receptor with AM-630, and SR-144528. Table 4 illustrates the residues predicted LPC data for CB2 complex.

The DASA studies are in agreement with the docking results (Table 4). As can be seen, there is a significant change

Table 3
Residues involved in binding sites of CB1 and CB2 receptors

Receptor	Residues first sphere (binding site) [a]	Residues first–second sphere [b]
CB1	Phe119, Lys122, Leu123, Val126, Phe130 [c], Pro181, Trp185, Asp196, Phe198, Trp209 [d], Ile210, Trp 286, Leu 289, Leu 290, Met 293	His73, Leu 95, Phe100, Phe 121, Lys122, Leu123, Gly125, Val 126, Ala128, Tyr154, Trp171, Phe198, Tyr205, Trp209, Val212, Leu218, Trp229, Val276, Lys300, Lys303, Asn319
CB2	Thr114, Met 115, Phe117 [c], Thr118, Ala 119, Val 121, Met157, Leu160, Ser161, Trp194 [d], Phe197, Phe 202	Leu39, Arg66, Phe91, Ser112, Val114, Thr 118, Leu160, Ser 161, Leu163, Pro176, Phe197, Phe202, His217, Lys279, Met293, Arg 302

[a] Residues involved in binding site (>3.6 Å), calculated with LPC program.
[b] Residues involved in first and second sphere of binding, calculated with DASA results.
[c] Phe 130 in CB1 corresponding to Phe 117 in CB2.
[d] Trp 209 in Cb1 corresponding to Trp 194 in CB2.

Table 4
Data of the docking study of CB1 and CB2 receptor

Ligand	HB [a]	Arom [b]	$E_{binding}$ [c]	k_i [d]
SR141716A [e]	O(CO)-Lys122	Phe130, Phe198	–64, 00	2.2 [53]
	N(2)-Trp209	Trp209, Trp286		5.9 [69]
AM-630 [f]	O-Thr114	Phe197	–39, 72	31.2 [54]
SR144528 [f]	N(1)-Ser165	Trp172, Tyr190	–67, 23	1.99 [70]
	N(2)-Ser165	Trp194, Phe197		5.6 [54]
	O(CO)-Ser161			
	N(NH)-Val164			

Underlined residues have been mutated.
[a] Hydrophilic–hydrophilic contact (hydrogen bond).
[b] Aromatic–aromatic contact.
[c] Energy of binding calculated with DOCK program (Sybyl).
[d] Human/cloned (CHO cells) ^{3}H-CP55940.
[e] Complex with CB1 receptor.
[f] Complex with CB2 receptor.

in the residues involved in the binding site. In addition, there are other residues which show an important change, suggesting that they may be involved the second sphere of interaction. Regarding to the interactions the results of the docking show that the antagonist AM630 and SR144528 interacts with CB2 receptor through a combination of HBs and aromatic interactions.

4. Conclusion

In conclusion, we have provided, the 3D models of the cannabinoid receptors CB1 and CB2 based on the highest resolution structure of a GPCR (1F88). The differences and analogies of both receptors have also been studied.

A model of the ligand–protein complexes are described by means of docking studies. The structural effects of ligand binding have been analyzed on the basis of hydrogen bond interactions, aromatic interactions and binding energy interactions in final complexes from manual docking and the FlexiDock program.

Docking studies reported here suggest that the binding process is governed through a combination of hydrogen bonding and aromatic interactions in both cannabinoid receptor CB1 and CB2.

Since the cannabinoid receptors CB1 and CB2 are interesting therapeutic targets, these studies of protein–ligand complexes can be very useful for the search of new compounds with cannabinoid properties. The design of novel ligands based on this cannabinoid receptor models are in progress.

Acknowledgements

The authors thank Emilia Bayo for her help in the transcription of this manuscript. This project is supported by the Ministerio of Ciencia y Tecnologia, Spain (SAF 2000-0114-C02-01) and Comunidad de Madrid (08.5/0050/2003 1).

References

[1] S.L. Palmer, G.A. Thakur, A. Makriyannis, Chem. Phys. Lipids 121 (2002) 3–19.
[2] A.C. Howlett, F. Barth, T.I. Bonner, G. Cabral, P. Casellas, W.A. Devane, C.C. Felder, M. Herkenham, K. Mackie, B.R. Martin, R. Mechoulam, R.G. Pertwee, Pharmacol. Rev. 54 (2002) 161–202.
[3] R.G. Pertwee, Prog. Neurobiol. 63 (2001) 569–611.
[4] P. Goya, N. Jagerovic, L. Hernandez-Folgado, M.I. Martin, Mini Rev. Med. Chem. 3 (2003) 765–772.
[5] C. Benito, E. Nunez, R.M. Tolon, E.J. Carrier, A. Rabano, C.J. Hillard, J. Romero, J. Neurosci. 23 (2003) 11136–11141.
[6] L. Volicer, M. Stelly, J. Morris, J. McLaughlin, B.J. Volicer, Int. J. Geriatr. Psychiatry 12 (1997) 913–919.
[7] A.S. Rice, Curr. Opin. Invest. Drugs 2 (2001) 399–414.
[8] F.P. Smith, Curr. Opin. Invest. Drugs 3 (2002) 859–864.
[9] G. Di Carlo, A.A. Izzo, Expert Opin. Invest. Drugs 12 (2003) 39–49.
[10] G.R. Pertwee, Pharmacol. Ther 95 (2002) 165–174.
[11] A.C. Porter, C.C. Felder, Pharmacol. Ther. 90 (2001) 45–60.

[12] R. Trillou, M. Le Arnone, C. Delgorge, N. Gonalons, P. Keane, J.P. Maffrand, P. Soubrie, J. Physiol. Regul. Integr. Comp. Physiol. 284 (2003) 345–353.
[13] J. De Vry, R. Schreiber, G. Eckel, K.R. Jentzsch, Eur. J. Pharmacol. 483 (2004) 55–63.
[14] P.J. McLaughlin, K. Winston, L. Swezey, A. Wisniecki, J. Aberman, D.J. Tardif, A.J. Betz, K. Ishiwari, A. Makriyannis, J.D. Salamone, Behav. Pharmacol. 14 (2003) 583–588.
[15] K. Zavitsanou, T. Garrick, X.F. Huang, Prog. Neuropsychopharmacol, Biol. Psychiatry 28 (2004) 355–360.
[16] M.E. Abood, B.R. Martin, Trends Pharmacol. Sci. 13 (1992) 201–206.
[17] L.A. Matsuda, S.J. Lolait, M.J. Brownstein, A.C. Young, T.I. Bonner, Nature 346 (1990) 561–564.
[18] S. Munro, K.L. Thomas, M. Abu-Shaar, Nature 365 (1993) 61–65.
[19] A. Chakrabarti, E.S. Onaivi, G. Chaudhuri, DNA Seq. 5 (1995) 385–388.
[20] C.M. Gerard, C. Mollereau, G. Vassart, M. Parmentier, Nucleic Acids Res. 18 (1990) 7142.
[21] C.M. Gerard, C. Mollereau, G. Vassart, M. Parmentier, Biochem. J. 279 (1991) 129–134.
[22] A. Calignano, G. La Rana, D. Piomelli, Eur. J. Pharmacol 419 (2001) 191–198.
[23] V. Di Marzo, C.S. Breivogel, Q. Tao, D.T. Bridgen, R.K. Razdan, A.M. Zimmer, et al., Neurochemistry 75 (2000) 2434–2444.
[24] N. Hájos, C. Ledent, T.F. Freund, Neuroscience 12 (2000) 3239–3249.
[25] Z.L. Lu, J.W. Saldanha, E.C. Hulme, Trends Pharmacol. 23 (2002) 140–146.
[26] R. Henderson, J. Baldwin, T.A. Ceska, F. Zenillin, E. Beckman, K.H. Downign, J. Mol. Biol. 213 (1990) 899–929.
[27] K. Palczewski, T. Kumasaka, T. Hori, C. Behnke, H. Motoshima, B. Fox, et al., Science 289 (2000) 739–745.
[28] P.L. Yeagle, G. Choi, A.D. Albert, Biochemistry 40 (2001) 11932–11937.
[29] D.C. Teller, T.C. Okada, A. Behnke, K. Palczewski, R.E. Stenkamp, Biochemistry 40 (2001) 7761–7772.
[30] L. Yeagle, G. Choi, A.D. Albert, Biochemistry 40 (2001) 11932–11937.
[31] SYBYL 6.9, Tripos Inc., 1699 South Hanley Rd., St. Louis, MO 63144, USA, 2002.
[32] D. Burke, C. Deane, H. Nagarajaram, N. Campillo, M. Martin-Martinez, J. Mendes, et al., Proteins 3 (1999) 55–60.
[33] J.D. Thompson, T.J. Gibson, F. Plewniak, F. Jeanmougin, D.G. Higgins, Nucleic Acids Res. 25 (1997) 4876–4882.
[34] N. Galtier, M. Gouy, C. Gautier, Comput. Appl. Biosci. 12 (1996) 543–548.
[35] K. Mizuguchi, C. Deane, T. Blundell, M.S. Johnson, J.P.J. Overington, Bioinformatic 14 (1998) 617–623.
[36] A. Sali, T.L. Blundell, J. Mol. Biol. 234 (1993) 779–815.
[37] A. Fiser, R.K. Do, A. Sali, Protein Sci. 9 (2000) 1753–1773.
[38] R. Luthy, J.U. Bowie, D. Eisenberg, Nature 5 (1992) 83–85.
[39] R.A. Laskowski, W. McArthur, D. Moss, J.M. Thornton, J. Appl. Crystallogr. 26 (1993) 283–291.
[40] A. Sali, T. Blundell, J. Mol. Biol. 20 (1990) 403–428.
[41] Z.Y. Zhu, A. Sali, T. Blundell, Protein Eng. 5 (1992) 43–51.
[42] M. Clark, R.D. Cramer III, N. Van Opdenbosch, J. Comp. Chem. 10 (1989) 982–1012.
[43] J.Y. Shim, W.J. Welsh, A.C. Howlett, Biopolymers 71 (2003) 169–189.
[44] A. Hurst, D.L. Lynch, J. Barnett-Norris, S.M. Hyatt, H.H. Seltzman, M. Zhong, Z.H. Song, J. Nie, D. Lewis, P.H. Reggio, Mol. Pharmacol. 62 (2002) 1274–1287.
[45] B.P. Gouldson, B. Calandra, P. Legoux, A. Kernéis, M. Rinaldi-Carmona, F. Barth, et al., Mol. Pharmacol. 401 (2000) 17–25.
[46] C.J.W. Huffman, R. Mabon, M.J. Wu, J. Lu, R. Hart, D.P. Hurst, P.H. Reggio, J.L. Wiley, B.R. Martin, Bioorg. Med. Chem. 11 (2003) 539–549.
[47] D.Q. Tao, S.D. Mcallister, J. Andreassi, K.W. Nowell, G.A. Cabral, D.P. Hurst, et al., Mol. Pharmacol. 55 (1999) 605–613.
[48] E.Z.H. Song, C.A. Slowey, D.P. Hurst, P.H. Reggio, Mol. Pharmacol. 56 (1999) 834–840.
[49] F.S.D. Mcallister, Q. Tao, J. Barnett-Norris, K. Buehner, D.P. Hurst, F. Guarnieri, P.H. Reggio, K.W. Nowell Harmon, G.A. Cabral, M.E. Abood, Biochem. Pharmacol. 63 (2002) 2121–2136.
[50] G.Z.H. Song, T.I. Bonner, Mol. Pharm. 49 (1996) 891–896.
[51] V. Sobolev, A. Sorokine, J. Prilusky, E.E. Abola, M. Edelman, Bioinformatics 15 (1999) 327–332.
[52] R. Judson, Genetic algorithms and their use in chemistry, in: K.B. Lipkowitz, D.B. Boyd (Eds.), Reviews in Computational Chemistry, vol. 10, VCH Publishers, New York, 1997, pp. 1–73.
[53] P. Gouldson, B. Calandra, P. Legoux, A. Kerneis, M. Rinaldi-Carmona, F. Barth, et al., Eur. J. Pharmacol. 401 (2000) 17–25.
[54] S.F. Altschul, T.L. Madden, A.A. Schaffer, J. Zhang, Z. Zhang, W. Miller, et al., Nucleic Acids Res. 1 (1997) 3389–3402.
[55] D.E. Garcia, S. Brown, B. Hille, K. Mackie, J. Neurosci. 18 (1998) 2834–2841.
[56] M. Caterina, M.A. Schumacher, M. Tominaga, T.A. Rosen, J.D. Levine, D. Julius, Nature 389 (1997) 816–824.
[57] H. Andersson, A.M. D'Antona, D.A. Kendall, G. Von Heijne, C.N. Chin, Mol. Pharmacol. 64 (2003) 570–577.
[58] A.C. Howlett, C. Song, B.A. Berglund, G.H. Wilken, J.J. Pigg, Mol. Pharmacol. 53 (1998) 504–510.
[59] D. Frishman, P. Argos, Protein Eng. 9 (1996) 133–142.
[60] D. Frishman, P. Argos, Proteins 27 (1997) 329–335.
[61] B. Rost, C. Sander, Proteins 20 (1994) 216–226.
[62] A.L. Ulfers, J.L. McMurry, D.A. Kendall, D.F. Mierke, Biochemistry 41 (2002) 11344–11350.
[63] D. Atmaram, A. Khanolkar, L. Palmer, A. Makriyannis, Chem. Phys. Lipids 108 (2000) 37–52.
[64] S. Bhattacharya, S. Ghosh, S. Chakraborty, A.K. Bera, B.P. Mukhopadhayay, I. Dey, A. Banerjee, BMC Struct. Biol. 1 (2001) 1472–6807.
[65] D. Shire, B. Calandra, M. Delpech, X. Dumont, M. Kaghad, G. Le Fur, et al., J. Biol. Chem. 271 (1996) 6941–6946.
[66] P.J. Kraulis, J. Appl. Crystallogr. 24 (1991) 946–950.
[67] D.J. Bacon, W.F.J. Anderson, J. Mol. Graph. 6 (1998) 219–220.
[68] E.A. Merrit, M. Murphy, Acta Crystallogr. 50 (1994) 869–873.
[69] C. Chin, J.W. Murphy, J.W. Huffman, D.A. Kendall, J. Pharmacol. Exp. Ther. 291 (1999) 837–844.
[70] J. Busch-Petersen, W.A. Hill, P. Fan, A. Khanolkar, X.Q. Xie, M.A. Tius, et al., J. Med. Chem. 39 (1996) 3790–3796.